



ELSEVIER

Journal of Chromatography A, 877 (2000) 95–107

JOURNAL OF
CHROMATOGRAPHY A

www.elsevier.com/locate/chroma

Study of the adsorption behavior of the enantiomers of 1-phenyl-1-propanol on a cellulose-based chiral stationary phase

Saad Khattabi^{a,c}, Djamel E. Cherrak^{b,c}, Jan Fischer^{b,d}, Pavel Jandera^d,
Georges Guiochon^{b,c,*}

^aDepartment of Food Science and Technology, The University of Tennessee, Knoxville, TN 37901-1071, USA

^bDepartment of Chemistry, The University of Tennessee, Knoxville, TN 37996-1600, USA

^cDivision of Chemical and Analytical Sciences, Oak Ridge National Laboratory, Oak Ridge, TN 37831-6120, USA

^dDepartment of Analytical Chemistry, University of Pardubice, Pardubice, Czech Republic

Received 12 May 1999; received in revised form 17 January 2000; accepted 25 January 2000

Abstract

Using single-step frontal analysis, we measured single-component and competitive adsorption isotherm data for the two enantiomers of 1-phenyl-1-propanol (PP). These experimental data were fitted to several competitive bi-Langmuir models (with 8, 6, 5 and 4 parameters) and to the competitive Langmuir model. The latter model accounted well for the behavior of both PP enantiomers on Chiracel OB (cellulose tribenzoate coated on silica gel). The parameters obtained were used in numerical calculations to predict the band profiles of the two single components and of their mixtures under overloaded conditions. The equilibrium-dispersive model provides satisfactory results, with minor differences between the calculated and the experimental profiles. These differences became negligible when a more complex kinetic model was used, with a concentration-dependent rate coefficient. © 2000 Elsevier Science B.V. All rights reserved.

Keywords: Enantiomer separation; Adsorption isotherms; Chiral stationary phases, LC; 1-Phenyl-1-propanol

1. Introduction

The demand for compounds with a high enantiomeric purity has kept increasing for the last few years, especially but not only for pharmaceuticals and pharmaceutical intermediates [1]. Because of the regulatory pressure regarding compounds existing as enantiomers [2] and also because of sometimes

profoundly different physiological activities of the two enantiomers, companies are looking into ways and means of economically producing relatively pure enantiomers. In that regard, enantioseparations using preparative liquid chromatography techniques proved cost effective compared to enantioselective synthesis. However, to uphold this advantage, chromatographic separations need to be optimized from both the production rate and the purity standpoints.

Effective and rapid optimization procedures may be easily carried out through modeling and computer simulation, resulting in considerable savings of time

*Corresponding author. Tel.: +1-865-9740-733; fax: +1-865-9742-667.

E-mail address: guiochon@utk.edu (G. Guiochon)

and money [3]. This theoretical approach is yet more critical when a sophisticated process such as simulated moving bed (SMB) is considered. Reaching steady-state in SMB after any parameter change takes typically several hours. This renders optimization through the conventional trial-and-error method a very expensive proposition. However, the modeling of any chromatographic process relies heavily on the preliminary determination of accurate adsorption isotherms [3]. In other words, the degree of accuracy of the modeling and of the predictions of the band profiles calculated from this model is directly related to the accuracy of the isotherm model itself and to that of its parameters. This illustrates the extreme care and attention that need to be given to the determination of the isotherm data.

The mechanism of enantioseparations on chiral stationary phases is not well understood. This in part due to the paucity of thermodynamic data available. For chiral phases on which the density of selective sites is low and these sites are isolated, the most widely accepted assumption is that the adsorbent surface is heterogeneous and contains two types of sites [3,4]. The first type are low-energy, non-selective sites. They are the most abundant ones and are characterized by fast mass transfer kinetics. They contribute significantly to the adsorption of both enantiomers but have no role in their separation. The second type of sites, essentially bonded ligands, are selective and responsible for chiral recognition, thus for the separation of the enantiomers. Those sites are characterized by a high adsorption energy and slow mass transfer kinetics which may cause important band broadening in some cases [3,4]. Cellulose-based phases are more complex, with a much higher density of enantioselective sites and conversely, a lower interaction energy. There are reasons to suspect that a more complex isotherm model is required [3].

The objective of this study was accurately to determine the quantitative isotherm behavior of 1-phenyl-1-propanol (PP) enantiomers on Chiracel OB (cellulose tribenzoate coated on silica gel), to use this result to predict the band profiles of single components and binary mixtures, and to investigate the mass transfer kinetics effect on the elution profiles.

2. Experimental

2.1. Equipment

2.1.1. HPLC system

All the experiments made for the isotherm determination were carried out with an HP 1090 liquid chromatograph (Hewlett-Packard, Palo Alto, CA, USA), equipped with a ternary-solvent delivery system, an automatic sample injector with a 250- μ l loop, a diode-array UV detector, and a computer data acquisition system using the HP-Chem-station software (version A.05.03). The acquired data were downloaded to one of the computers at The University of Tennessee Computer Center for further data processing.

2.1.2. Preparative chromatograph

For the purification of the racemic mixture, an LC-50 dynamic axial compression system skid (Prochrom, Champineulles, France) was used. The 50 mm I.D. column was operated with a Dynamax SD-1 dual-piston pump (Rainin, Woburn, MA, USA).

2.2. Materials

2.2.1. Column

In all the experiments, we used a 20 cm \times 1.0 cm I.D. column, packed in-house with Chiracel OB (cellulose tribenzoate coated on a silica gel substrate, 20 μ m particles) from Daicel (Tokyo, Japan). The total porosity ($\epsilon_T=0.734$) was determined by injecting a non-retained compound (1,3,5-tri-*tert*-butyl benzene, $t_0=4.61$ min at a flow-rate of 2.5 ml/min). The efficiency of the column ($N=1200$ plates) was determined for non-retained TTBB, from the width of the peak at half height. At infinite dilution, k' was 1.19 for S-PP and 1.57 for R-PP and the selectivity factor was $\alpha=1.32$.

2.2.2. Mobile phase and chemicals

HPLC grade *n*-hexane and ethyl acetate were purchased from Fisher Scientific (Fair Lawn, NJ, USA). 1,3,5-tri-*tert*-butyl benzene (TTBB), S-PP, R-PP and the racemic mixture of PP were obtained from ALDRICH (Milwaukee, WI, USA). Although the PP products (S-, R-, and the racemic mixture)

were more than 99% pure, the products received from the manufacturer contained an impurity that absorbed significantly at the chosen wavelengths (254 and 270 nm). This impurity was removed by preparative liquid chromatography on a 28.5 cm×5 cm column packed with C₁₈-bonded silica Impaq (BTR separation, Wilmington, DE, USA), with isopropanol as the mobile phase. The product obtained was free from the UV-absorbing impurity. Small amounts (1 ml each) of the two pure enantiomers were purified by preparative HPLC using a semi-preparative column (25 cm×1 cm), packed with the same stationary phase.

2.3. Procedures

All experiments were performed with a *n*-hexane–ethyl acetate (95:5, v/v) solution as the mobile phase at room temperature (22–24°C). Note that the stationary phase becomes unstable if the ethyl acetate concentration exceeds 5%. Changes in the concentration of ethyl acetate in the mobile phase caused only a moderate variation of the separation factor of the two enantiomers. The temperature was periodically monitored. The flow-rate was 2.5 ml/min, unless otherwise indicated.

2.3.1. Determination of adsorption isotherm for single component

The adsorption isotherm data for the PP enantiomers were measured using single-step frontal analysis. Two compartments of the solvent delivery system were used. One (reservoir A) was filled with the pure mobile phase. The other compartment (reservoir B) was filled with a solution of one enantiomer. In all experiments, the column was first equilibrated with pure mobile phase, prior to injecting a large volume sample (ca. 15 ml). This injection results into the elution of a breakthrough curve followed by a concentration plateau corresponding to the elution of the injected mixture, after equilibrium is reached. Then the sample pulse is washed off the column and, before the next injection, the column flushed with pure mobile phase until equilibrium is reached again. This procedure is tedious and time consuming but has the advantage over the conventional staircase mode that cumulative errors in

isotherm calculation are avoided. Each successive pulse injected contains 5, up to 20%, and then 10% more solution B than the previous one. The last one was obtained with 100% solution B (5.6 g/l for S-PP and 5.43 g/l for R-PP).

The UV detector was calibrated at 270 nm. The UV-absorbance data were transformed into concentrations by averaging the measurements made on each plateau. The slightly nonlinear calibration curve was fitted to a second-degree polynomial. Due to the achiral nature of the UV response, the same calibration curve was used for both enantiomers.

The amount of each compound adsorbed by the stationary phase at equilibrium were determined from the elution time of the inflection point of the breakthrough curve through the classical equation [5]:

$$q = \frac{C(V_F - V_0)}{V_a} \quad (1)$$

where q is the amount adsorbed on the solid phase in equilibrium with the concentration C in the mobile phase, V_F is the retention volume of the inflection point of the breakthrough curve, V_0 is the column void volume, and V_a is the volume of adsorbent in the column.

2.3.2. Determination of competitive adsorption isotherm.

The competitive adsorption isotherms were measured using the single-step binary frontal analysis method [5]. The two compartments of the pump were filled, one (A) with the pure mobile phase and the other (B) with a solution of racemic PP (total concentration 6.6 g/l). In all experiments, the column was equilibrated with pure mobile phase prior to injecting a large volume plug (ca. 15 ml) of diluted solution B. The elution signal has two successive steps, one of pure less retained compound (S enantiomer), the other of injected solution. There is no need to analyze the relative concentration of the two enantiomers in the intermediate plateau since it contains exclusively the first enantiomer [5]. The concentration of S-PP at the intermediate plateau was derived from the calibration curve at 270 nm and the plateau height. The adsorbed amount of each en-

antimer in the mixture, q_x , was derived from the retention volumes of the two breakthrough curves and their corresponding concentrations, C_x , using the equation given by Jacobson et al. [5]:

$$q_x = \frac{C_x(V_{S+R} - V_0) - C_{x,ip}(V_{S+R} - V_S)}{V_a} \quad (2)$$

where V_0 , V_{S+R} , V_S , and V_a are the column holdup volume, the elution volumes of the two breakthrough fronts, and the volume of adsorbent in the column, respectively; $x=R$ or S ; $C_{R,ip} = 0$; and $C_{S,ip}$ is the concentration of the S enantiomer at the intermediate plateau.

2.3.3. Fitting the isotherm data to the isotherm model

The experimental adsorption data were fitted to the Langmuir and the bi-Langmuir isotherm models, the latter with 8, 6 and 4 parameters (see later). The best values of the coefficients of these models were calculated using a nonlinear regression program (Sigma Plot 4.00, SPSS Inc., San Rafael, CA, USA). The best coefficients for the isotherm parameters were obtained by minimizing the following function:

$$\sigma^2 = \sum_{i=1}^{N_d} \left(\frac{q_i^{\text{exp}} - q_i^{\text{th}}}{q_i^{\text{th}}} \right)^2 \quad (3)$$

where N_d is the number of data points, and q_i^{exp} and q_i^{th} are the experimental and the calculated data points, respectively. In the regression, the experimental data were given a weight equal to $1/q_{\text{experimental}}$ to account for the nearly constant relative error made in the measurement of the amounts adsorbed at equilibrium. The values of the objective function obtained when the experimental data are

fitted to different models are listed in Tables 1 and 2. The quality of the fit is represented by the PRESS coefficient (Predicted Residual Error Sum of Squares) [6]. The smaller this coefficient, the better the predictive ability of the model. For the different competitive isotherm models investigated in this work, except for the 8-parameter bi-Langmuir model, PRESS predictably increased with decreasing number of the model parameters. For the 8-parameter model, the much higher PRESS may be explained by a problem of multicollinearity which appears when the number of parameters allowed is excessive for the set of data (i.e. because of its range, of the accuracy of the data, and/or the actual need for a complex model). The regression program affords also the standard error also tabulated as the relative standard deviation (RSD) made on the best estimate of the parameters (see Tables 1 and 2). This precision must also be taken into account when selecting the best model for a given set of data.

3. Theory

3.1. Band profile calculations

The band profiles were calculated using two models of nonlinear chromatography, the equilibrium-dispersive model and the lumped kinetic model.

3.1.1. Equilibrium-dispersive model

This model assumes instantaneous equilibrium between the stationary and the mobile phase and integrates the differential mass balance equation for the two components of the mixture, taking the isotherm equations into account. To account for the

Table 1
Single component isotherm coefficients for 1-phenyl-1-propanol enantiomers^a

# Para	Site	Isomer	a	SE	RSD (%)	b (1/g)	SE	RSD (%)	q_s (g/l)	PRESS
Bilang	ns	S	2.65	0.03	1.03	0.049	0.001	2.9	54.7	0.49
		R	3.57	0.09	2.42	0.060	0.003	4.5	51.8	0.004
	s	S	0.49	0.02	3.47	1.397	0.238	17.1	0.35	
		R	0.63	0.07	10.7	0.975	0.253	25.9	0.65	
Lang		S	2.91	0.02	0.71	0.066	0.003	3.8	44.2	0.19
		R	3.99	0.02	0.58	0.09	0.002	2.4	44.4	0.51

^a The experimental data were fitted to the Langmuir $\left(q_i = \frac{aC_i}{1 + bC_i} \right)$ and to the bi-Langmuir model $\left(q_i = \frac{a_{ns}C_i}{1 + b_{ns}C_i} + \frac{a_sC_i}{1 + b_sC_i} \right)$.

Table 2
Competitive isotherm coefficients for 1-phenyl-1-propanol enantiomers^a

# Para	Site	Isomer	<i>a</i>	SE	RSD (%)	<i>b</i> (l/g)	SE	RSD (%)	<i>q_s</i> (g/l)	PRESS
8p	ns	S	2.14	1.55	72.54	0.122	0.068	55.15	17.5	209
		R	2.889	2.10	72.55	0.175	0.109	62.17	16.5	
	s	S	0.855	1.56	182.33	0	0.075	*	*	
		R	1.3	2.11	172.17	0	0.090	*	*	
6p	ns	S	2.93	*		0.0647	0.002	3.40	45.4	1.42
		R								
	s	S	0	*		0	0.014	*	*	
		R	1.16	*		0.237	0.021		4.9	
5p	ns	S	2.93	*		0.0647	0.002	3.40	45.4	1.76
		R								
	s	S	0	*		0	0.008	*	*	
		R	1.16	*		0.237	0.022	9.31	4.9	
4p (S-lang)	ns	S	2.93	0.02	0.62	0.0647	0.002	2.94	45.3	3.06
R (Bi-lang)		R								
	s	S	*	*		*	*			
		R	1.16	*		0.237	0.020	8.55	4.89	
Langmuir		S	2.97	0.03	0.94	0.0644	0.003	5.12	46.0	496.2
		R	3.96	0.04	0.90	0.0804	0.003	4.23	49.2	

^a Competitive Langmuir model:

$$q_1 = \frac{a_1 C_1}{1 + b_1 C_1 + b_2 C_2} \quad q_2 = \frac{a_2 C_2}{1 + b_1 C_1 + b_2 C_2}$$

Competitive bi-Langmuir model with eight parameters

$$q_1 = \frac{a_{ns1} C_1}{1 + b_{ns1} C_1 + b_{ns2} C_2} + \frac{a_{s1} C_1}{1 + b_{s1} C_1 + b_{s2} C_2} \quad q_2 = \frac{a_{ns2} C_2}{1 + b_{ns1} C_1 + b_{ns2} C_2} + \frac{a_{s2} C_2}{1 + b_{s1} C_1 + b_{s2} C_2}$$

For 6 parameter model: $a_{ns1}/b_{ns1} = a_{ns2}/b_{ns2}$. For 5 parameter model: $a_{ns1}/b_{ns1} = a_{ns2}/b_{ns2}$ and $a_{s1}/b_{s1} = a_{s2}/b_{s2}$.

finite column efficiency, an apparent dispersion coefficient, D_a , is used instead of the axial dispersion coefficient which would account for axial and eddy dispersion. The axial dispersion coefficient is assumed constant and equal to its value under linear conditions:

$$D_a = \frac{u_o L}{2N} \quad (4)$$

where u_o is the mobile phase velocity, L the column length, and N the number of theoretical plates. This model is valid when the band profile is more influenced by the nonlinear behavior of the equilibrium isotherm than by kinetic effects. this is so because all contributions to band broadening are

lumped together into the single apparent axial dispersion coefficient, D_a [3].

3.1.2. Lumped kinetic model (transport-equilibrium)

In this study, the solid film linear driving force model was used to account for the mass transfer kinetics [3]. This model assumes that the rate of variation of the stationary phase concentration, $\partial q/\partial t$, is proportional to the difference between the concentration of the compound in the stationary phase at equilibrium with the concentration C in the mobile phase, q^* , and the actual concentration, q . The proportionality coefficient, k_f (min^{-1}), is the mass transfer rate coefficient. The combination of

this rate equation and the mass balance equation constitutes the transport-dispersive model [3]. This model still includes an axial dispersion coefficient. Its value was set constant (see later) and the mass transfer coefficient was derived by identification of the experimental profile to a numerical solution of the model. Numerical solutions can be obtained using an appropriate program [3].

3.1.3. Boundary conditions

These conditions characterize the experiment performed. Initially the column was free of sample, containing only the stationary phase in equilibrium with pure mobile phase. We used the classical boundary conditions of elution chromatography corresponding to the injection of a rectangular pulse of known width and maximum concentration. Injection profiles obtained for three different volumes (0.5, 1 and 2 ml) are shown in Fig. 1. They validate the assumption of a rectangular pulse injection.

4. Results and discussion

4.1. Modeling of the single component equilibrium isotherms

The single component isotherm data obtained for each enantiomer were fitted to the Langmuir and the bi-Langmuir models. Fig. 2 compares the experimental data (symbols) and the best fitted Langmuir model (dashed line). This model fits the data well, as well as the bilangmuir model (results not shown). The reasons for its selection are as follows. First, the statistical data are shown in Table 1. They include the best values of the parameters for each model, their absolute (SE) and relative standard deviations (RSD). These data indicate that the qualities of the two fits are comparable, with similar values of PRESS and of the RSD of the different parameters (except for the parameters of the second Langmuir term). Second, the Scatchard plots of the data are shown in Fig. 3 (symbols for experimental data, solid

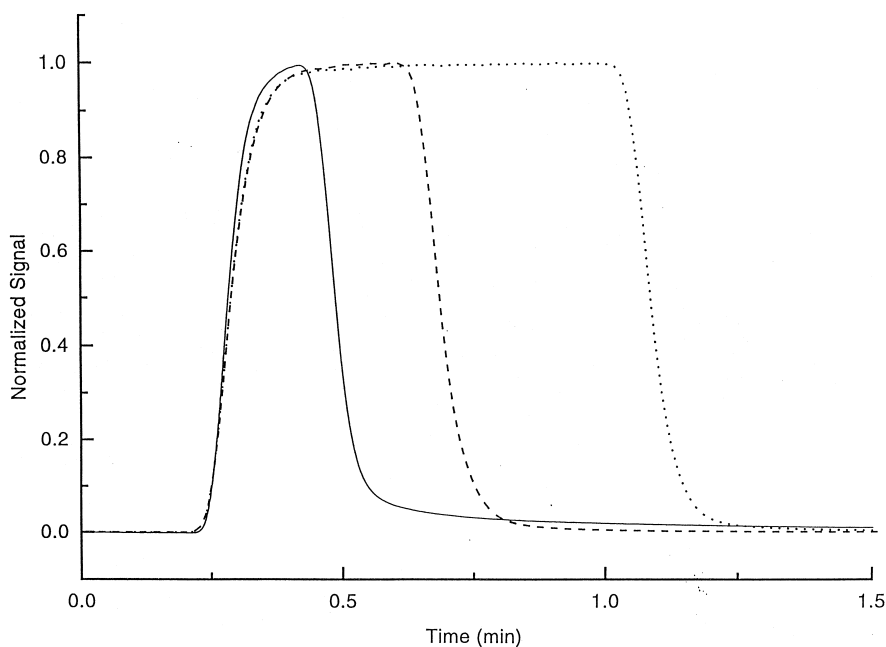


Fig. 1. Injection profiles of increasing volumes of a racemic PP solution, without column. Solid line: 0.5 ml, dashed line: 1.0 ml, dotted line: 2.0 ml.

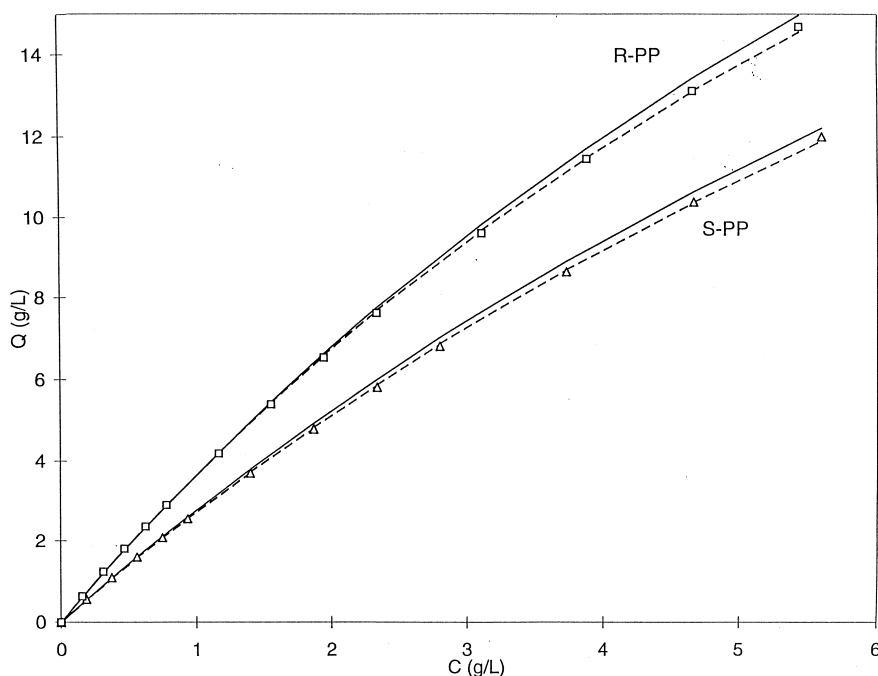


Fig. 2. Single component experimental data (symbols: Δ =S-PP, \square =R-PP) for the 1-phenyl-1-propanol enantiomers on Chiracel OB. Experimental data (symbols): Langmuir isotherms calculated with the best coefficients given by the regression of the experimental data to the Langmuir model (dashed lines), and Langmuir isotherms calculated with the coefficients derived from the regression of the combined competitive and single component data (solid lines). Column: length, 200 mm; I.D., 10 mm. Mobile phase: *n*-hexane–ethyl acetate, 95:5, v/v; flow-rate=2.5 ml/min. The mobile phase concentration ranged approximately from 0.18 to 5.6 g/l for S-PP and from 0.15 to 5.4 g/l for R-PP.

lines for the best Langmuir model). They exhibit a near linear relationship, consistent with a Langmuir model [3,7]. The data at low concentrations may suggest the possibility of a second term, with a small saturation capacity. The statistical data in Table 1 show that the improvement obtained by adding a second Langmuir term is not significant, the RSD values on the model coefficients being slightly lower with the Langmuir model than with the bi-Langmuir one and the PRESS hardly changed. So, the Langmuir model appears to be preferable for the sake of simplicity. Finally, as results from the discussion of the results obtained in fitting the competitive isotherm data (see later), the Langmuir model is also more satisfactory than the bilangmuir model.

The solid line in Fig. 2 shows the single component isotherms calculated from the set of co-

efficients obtained by fitting together the experimental data obtained in both the single-component and the competitive adsorption measurements to the competitive Langmuir model. Although the agreement is slightly less good (as happens in most similar cases [3]), it still remains better than satisfactory. This result suggests that it is possible, at least in some cases, to predict reasonably well the single component isotherm from the measurements of competitive isotherm data measured only with the racemic mixture.

4.2. Modeling of the competitive equilibrium isotherms

Even though the fit of single-component data suggested the Langmuir model to be more appro-

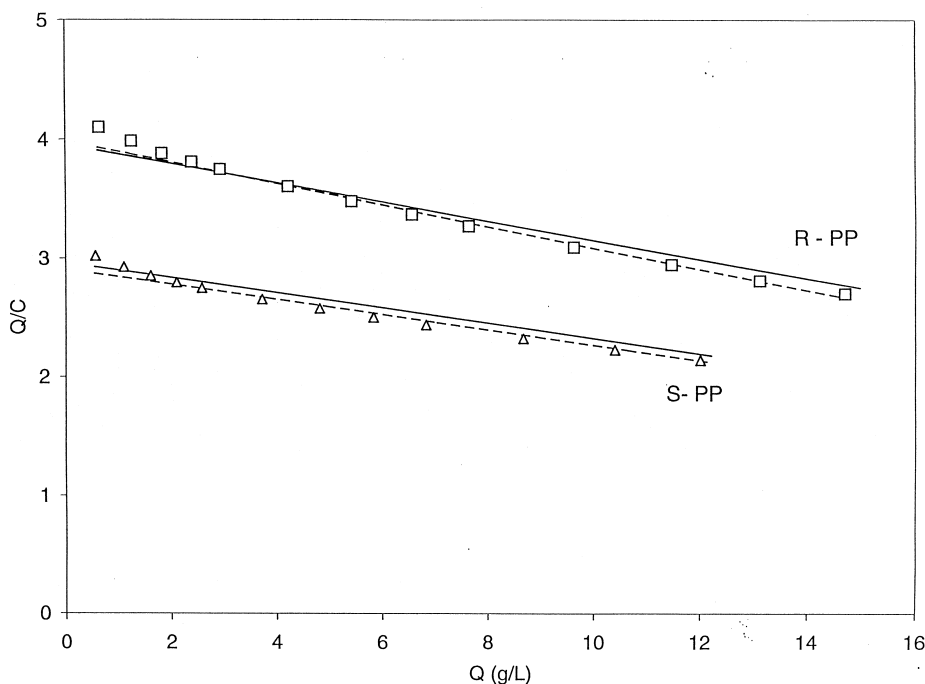


Fig. 3. Scatchard plots of the experimental adsorption data (symbols: Δ =S-PP, \square =R-PP) of the enantiomers of 1-phenyl-1-propanol. The lines correspond to the isotherms calculated with the same coefficients as used for the corresponding lines in Fig. 1, coefficients derived from single component data (dashed lines) and coefficients derived from combined competitive and single component data (solid lines).

appropriate, the competitive and the single-component data were fitted together to both models. The competitive bi-Langmuir models with 8, 6, 5 and 4 parameters were investigated. The 8 parameter model allows both selective and non-selective types of sites to differ for the two enantiomers, an unlikely situation which would assume cooperative interactions of these two types of sites. The more physically sound 6-parameter model assumes the nonselective sites to be the same for both enantiomers, while the 5-parameter model assumes further that the saturation capacity of the chiral sites are the same for both enantiomers ($q_{\text{chiral}} = a_s/b_s = a_r/b_r$). This is often the case for stationary phases made of bonded proteins [3,4]. Finally, the 4-parameter model assumes that one of the two enantiomers does not interact with the selective sites. In this case, the model simplifies to a Langmuir term for this enantiomer and remains a bi-Langmuir model for the other one. This last model was successfully used to describe the adsorption behavior of the phenyl-alanine anilide enantiomers on imprinted polymeric stationary phases [8].

The results obtained by fitting all the adsorption data to these different models are summarized in Table 2. The 8-parameter model is the least appropriate, not only generating large RSD values for all coefficients but also estimating the coefficient b of both enantiomers on the selective site to be zero, hence its saturation capacity to be infinite (Table 2). All other three bi-Langmuir models generated almost exactly the same estimates for the non-selective site parameters (2.93 for a_{ns} , 0.065 for b_{ns}) and for the selective site parameters for the R enantiomer ($a_r = 1.162$ and $b_r = 0.237$). Finally, all three models estimate the selective site capacity factor for the S enantiomer to be zero (Table 2), making all these models equivalent to the simpler 4-parameter bi-Langmuir model. As expected, the saturation capacity was found to be much larger (10-fold) for the non-selective than for the selective sites.

The data fitted nearly as well to a simple competitive Langmuir model (Table 2). The precision on the model parameters (SE or RSD), was comparable for the Langmuir and the last three bi-Langmuir models

(i.e. the RSD values for comparable parameters were similar). Given the greater simplicity of the Langmuir model, it seems to be the best choice in spite of its larger PRESS value. Fig. 4 compares the experimental data points for the competitive isotherms measured with the racemic mixture (symbols: (\square) R-PP, (\triangle) S-PP) and the isotherms calculated with the Langmuir model and two sets of coefficients. The first set was derived from the competitive data only (dashed line). A comparison between the symbols and the dashed lines illustrates the sensitivity of the PRESS value to small deviations of the experimental data from the model. The second set was obtained by fitting together the competitive and the single-component data (solid line). There is an excellent agreement between the experimental data and the two sets of isotherms, similar to the one observed in Fig. 2. Finally, note that the saturation capacities for the two enantiomers (46.05 for S-PP and 49.23 for R-PP) are very close, which makes the model nearly thermodynamically consistent.

Table 3 displays the isotherm coefficients derived from the single component data, the competitive

Table 3

Comparison of simple competitive Langmuir isotherm coefficients determined from single component data, competitive data and the combination of both^a

	a (S)	b (S) (1/g)	a (R)	b (R) (1/g)
Single alone	2.909	0.066	3.99	0.09
Comp. alone	3.098	0.066	4.09	0.088
Combined	2.97	0.064	3.96	0.080

^a Single component data alone: coefficients derived from the single component data only. Competitive data alone: coefficients derived from the competitive data only. Combined data: coefficients derived from the combined competitive and single component data.

data, and the combined set of data. The three sets of best coefficients afforded by the regression are very close. This agreement, which is also illustrated in Figs. 2 and 4, is an important result. If confirmed for other racemic mixtures and phase systems, it would be very valuable, allowing major savings in time and money for the determination of the competitive isotherm data required for the successful modeling of enantiomeric separations.

Similar results, with the Langmuir model account-

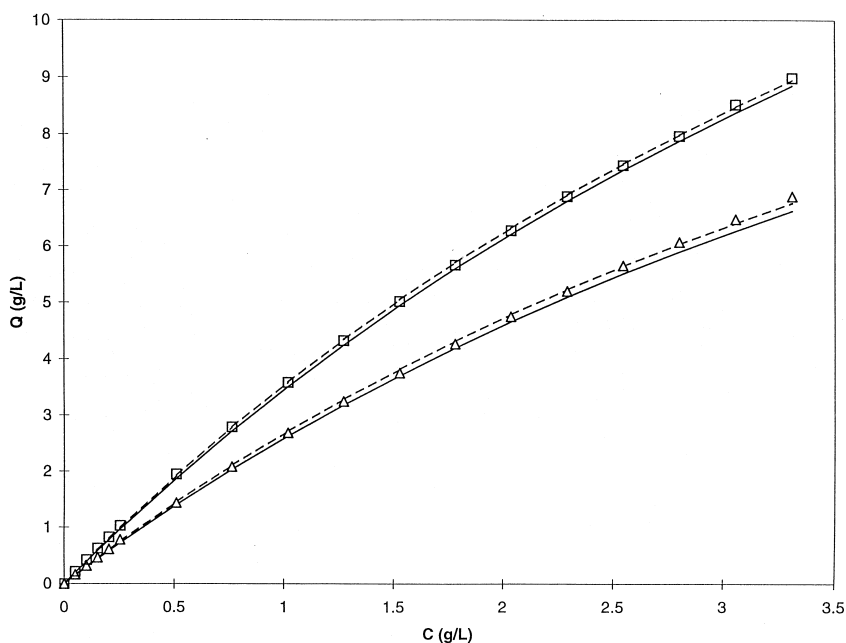


Fig. 4. Experimental competitive adsorption data (symbols: \triangle = S-PP, \square = R-PP). Symbols, experimental data. The lines are the isotherms calculated with the coefficients derived from the competitive data alone (dashed lines) and with those derived from the combined competitive and single component data (solid lines). See Fig. 2 for experimental conditions.

ing best for the adsorption behavior of the two enantiomers of 3-chloro-1-phenyl-1-propanol on the same chiral stationary phase, were recently obtained by Cherrak et al. [9]. These results contrast with other previously reported studies in which the bi-Langmuir model was shown to be the model of choice [3,4,10]. Jacobson et al. measured the equilibrium isotherms of four pairs of enantiomers (mandelic acid, tryptophan, phenyl-butyric acid and *N*-benzoyl-alanine) on bovine serum albumin bonded to silica [3]. Charton et al. [10] examined the behavior of methyl-mandelate and of ketoprofene on immobilized cellulose tribenzoate. Fornstedt et al. [4] investigated the adsorption behavior of the enantiomers of propranolol on the protein CBH I immobilized on silica. More recently, Pais et al. [11] proposed a model simpler than the bi-Langmuir model, the sum of a linear and a Langmuir term, to account for the behavior of epoxide enantiomers on microcrystalline cellulose tri-acetate. Finally, Chen et al. [8] were able to use the 4-parameter bi-Langmuir model to explain the adsorption of the enantiomers of phenyl-anilide on an imprinted polymeric stationary phase.

4.3. Validation of the isotherm model

In the modeling of chromatographic processes, a model is only as good as its ability to predict band profiles, not only for the single components but, most importantly, for binary mixtures, regardless of their absolute or relative concentrations. Finding a suitable model that fits well experimental data is relatively easy but a model is valid only if it can be used adequately to predict band profiles. This is why it must be validated.

4.3.1. Single component band profiles

Band profiles were calculated using the best values of the parameters of the competitive Langmuir model (Table 2). Fig. 5a,b compare the experimental band profiles (symbols) obtained for two samples of different volumes (1 and 2 ml, respectively) of an S-PP solution (9.335 g/l) and the profiles calculated with different models and conditions. A fair agreement was observed between the experimental profile and the profiles given by the equilibrium-dispersive model (dashed line). The main differences are more diffuse front and rear parts of the experimental

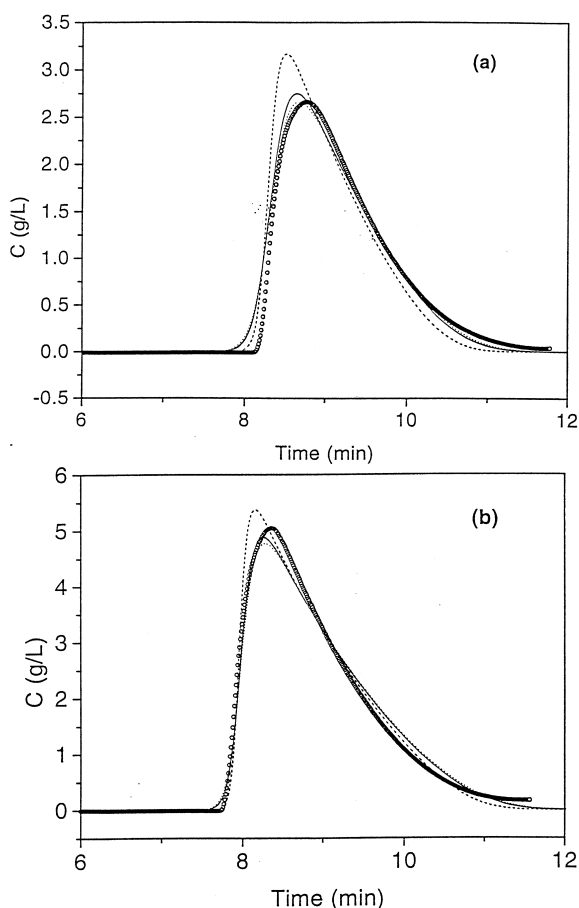


Fig. 5. Experimental (symbols) and calculated elution profiles for increasing volumes for S-PP solution ($C=9.335 \text{ g/l}$). Injection volume: (a) 1.0, (b) 2.0 ml. Equilibrium-dispersive model (dashed lines) and transport-dispersive model (solid lines: $k_t=150 \text{ min}^{-1}$, dotted line: $k_t=80 \text{ min}^{-1}$).

profile which is also shorter. This suggests that the assumption of a fast mass transfer kinetics may not hold entirely true. The diffuse rear part of the profile exhibits a degree of tailing which might be due to a relatively slow mass transfer kinetics [3]. The other two profiles in Fig. 5a,b were calculated with the transport-dispersive model. In the application of this model, it was assumed that the axial dispersion coefficient of this model was equal to half the value of the apparent axial dispersion coefficient used for the equilibrium-dispersive model (and corresponding to an efficiency of 1200 theoretical plates). The profiles shown in the figures were obtained for

values of the rate coefficient of 80 (dotted lines) and 150 (solid lines) min^{-1} . The best agreement was obtained with $k_f = 80 \text{ min}^{-1}$.

Similar results were obtained for the R enantiomer (7.764 g/l solution). Fig. 6a,b compare experimental and calculated profiles. The profiles given by the equilibrium-dispersive model (dashed line) agree only fairly well with the corresponding experimental profiles (symbols). An excellent agreement is with the profiles given by the transport-dispersive model. The best agreement was obtained for $k_f = 60 \text{ min}^{-1}$ (dotted line) in both cases. As expected, k_f was found to be lower for the more retained enantiomer (R-PP), albeit only slightly so.

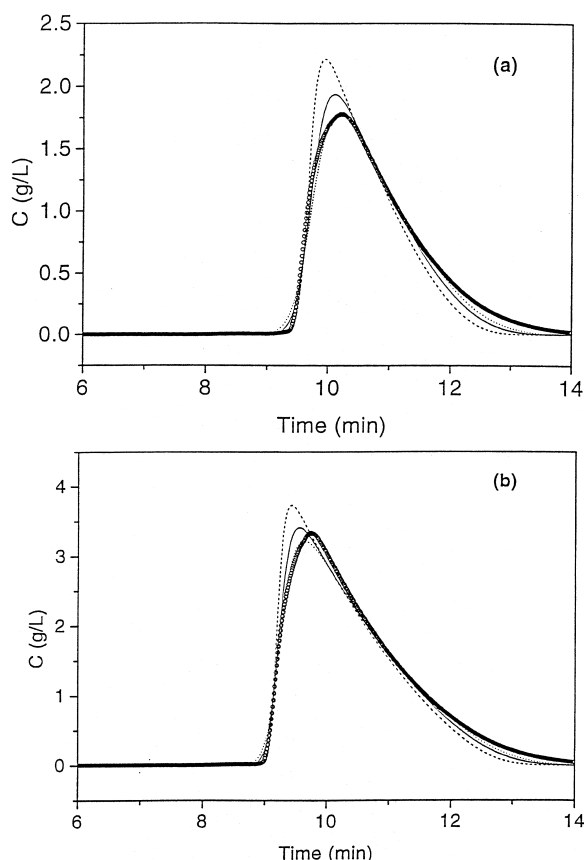


Fig. 6. Experimental (symbols) and calculated elution profiles for increasing volumes for R-PP solution ($C = 7.764 \text{ g/l}$). Injection volume: (a) 1.0, (b) 2.0 ml. Equilibrium-dispersive model (dashed lines) and transport-dispersive model (solid lines: $k_f = 150 \text{ min}^{-1}$, dotted line: $k_f = 60 \text{ min}^{-1}$).

4.3.2. Band profiles for binary mixtures

To further validate the model selected, the band profiles of samples of the racemic mixture of increasing sizes were calculated with the isotherm parameters of the Langmuir model and compared to experimental results. Fig. 7a,b,c,d illustrate such comparisons for 0.25, 0.5, 1 and 2 ml samples of a 10.62 g/l solution of the racemic mixture. The dotted lines show the profiles calculated with the transport-dispersive model and a rate coefficient $k_f = 10\,000 \text{ min}^{-1}$ for both enantiomers. The dashed lines are the profiles calculated with the same values of k_f as optimized for the single component profiles (Figs. 5 and 6), namely 80 min^{-1} for S-PP and 60 min^{-1} for R-PP. Finally the rate coefficients were adjusted in each case to obtain the best possible agreement between calculated and experimental profiles (solid lines). The profiles calculated with high values of the rate coefficients ($10\,000 \text{ min}^{-1}$) do not agree well with the experimental profiles at low concentrations (Fig. 7a,b). They agree better at higher concentrations (Fig. 7c,d). This confirms the concentration dependence of the mass transfer rate coefficient previously reported [3,7,12].

This conclusion is confirmed by the comparison between the solid line profiles which were calculated with values of k_f different for each sample size, in an effort to match as well as possible each experimental profile with a numerical solution of the transport-dispersive model. This best agreement was obtained with values of k_f increasing with increasing injection volume ($k_{f1} = 150, 300, 500$ and 1000 min^{-1} ; $k_{f2} = 60, 80, 120$ and 300 min^{-1} , for $V_{inj} = 0.25, 0.5, 1$ and 2 ml , respectively). This agreement between calculated and experimental profiles was much better than when values of k_f equal to those used to optimize the agreement between experimental and calculated profiles of single components were used (dashed lines). This suggests a possibility that the rate coefficients could be competitive under certain circumstances.

5. Conclusion

The results of this study confirm that there are many cases in which the simple Langmuir isotherm model can be used satisfactorily to account for the adsorption behavior of two enantiomers. Because of

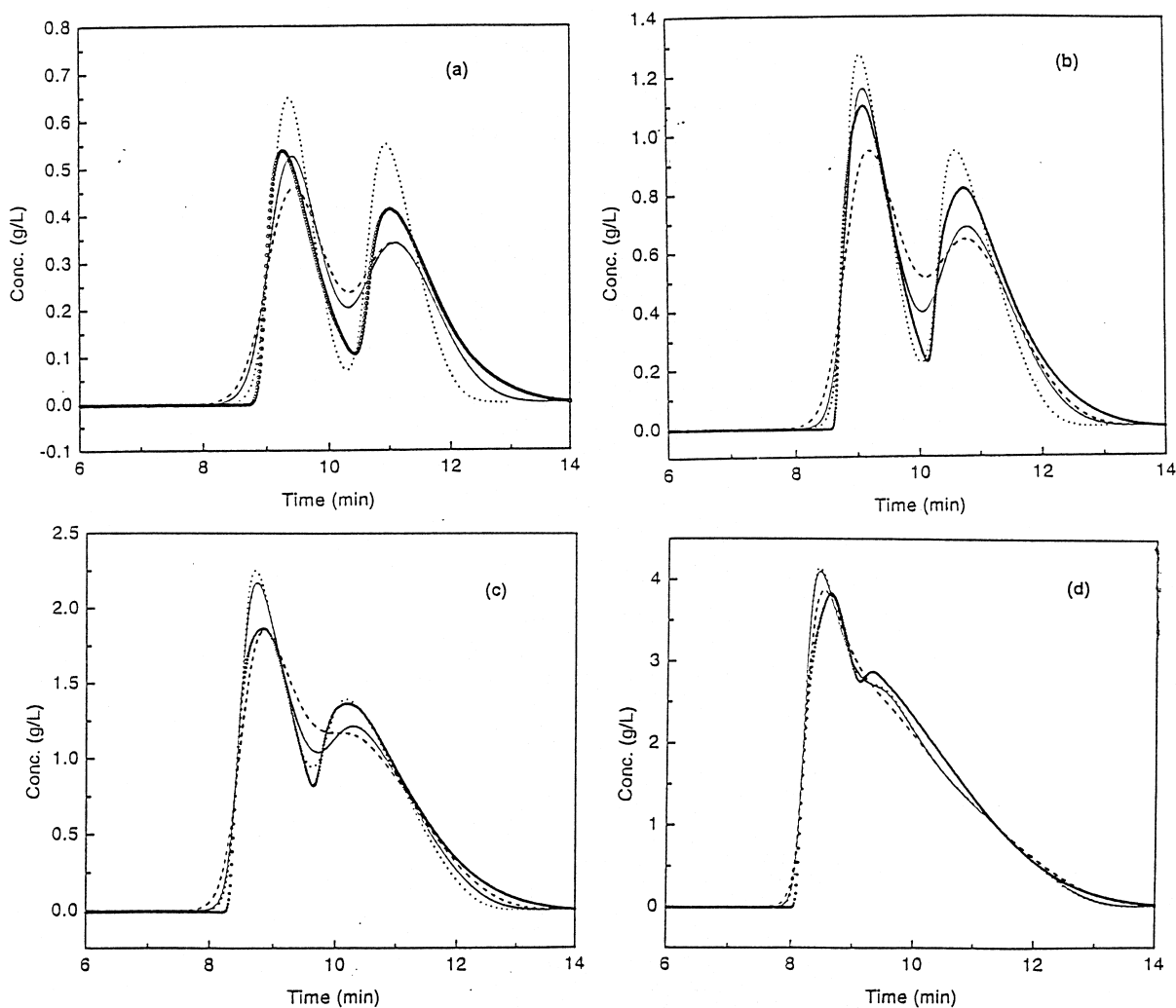


Fig. 7. Experimental (symbols) and calculated elution profiles for increasing volumes of the racemic mixture of PP (total concentration = 10.62 g/l) solution. Injection volume: (a) 0.25, (b) 0.5, (c) 1.0 and (d) 2.0 ml. Profiles were calculated with the transport-dispersive model for different values of k_r . In all four figures, dotted lines: $k_{r1} = k_{r2} = 10\,000\text{ min}^{-1}$; dashed lines: $k_{r1} = 80\text{ min}^{-1}$, $k_{r2} = 60\text{ min}^{-1}$. Solid lines: (a) $k_{r1} = 150\text{ min}^{-1}$, $k_{r2} = 60\text{ min}^{-1}$; (b) $k_{r1} = 300\text{ min}^{-1}$, $k_{r2} = 80\text{ min}^{-1}$; (c) $k_{r1} = 500\text{ min}^{-1}$, $k_{r2} = 120\text{ min}^{-1}$; (d) $k_{r1} = 1000\text{ min}^{-1}$, $k_{r2} = 300\text{ min}^{-1}$.

the known relationship between adsorption energy distribution and isotherm model [13,14], this suggests that, in these cases, the spectrum of interaction energies between the molecules of either of the two enantiomers of the analyte and those of the stationary phase is relatively narrow. In the present case, this conclusion is justified by the fact that the molecules of the cellulose-based stationary phase have a high

density of atoms existing only under one of the two possible chiral conformations. Further conclusions on the chiral separation mechanism require, however, more detailed investigations of the origin of the considerable variations in the separation factor (including possible inversion of the elution order) caused by changes in the composition of the mobile phase or the nature of the strong solvent selected.

Acknowledgements

This work was supported in part by Grant CHE-97-01680 of the National Science Foundation, by the project No. 150 of the Czech Ministry of Education and the National Scientific Foundation, and by the cooperative agreement between the university of Tennessee and the Oak Ridge National Laboratory. The authors are grateful to Chiral Technologies (Exton, PA, USA) for the generous gift of Chiracel OB stationary phase and to Prochrom (Champigneulle, France) for the loan of the LC-50 dynamic axial compression system used in this work.

References

- [1] S.C. Stinson, Chemical and Engineering News, C.&E.N., 73 (Oct. 9) (1995) 44.
- [2] Anon., FDA's policy statement, Chirality 4 (1992) 338.
- [3] G. Guiochon, S. Golshan-Shirazi, A.M. Katti, Fundamentals of Preparative and Nonlinear Chromatography, Academic Press, Boston, MA, 1994.
- [4] T. Fornstedt, G. Zhong, Z. Bensetiti, G. Guiochon, Anal. Chem. 68 (1996) 2370.
- [5] J. Jacobson, J.H. Frenz, Cs. Horváth, Ind. Eng. Chem. Res. 26 (1987) 43.
- [6] SigmaPlot 4.0, Manual of Instructions, SPSS, San Rafael, CA, 1997.
- [7] J.D. Andrade (Ed.), Surface and Interfacial Aspects of Biomedical Polymers, Plenum Press, New York, 1985, p. 60, Chapter 1.
- [8] Y. Chen, M. Kele, P. Sajonz, B. Sellergren, G. Guiochon, Anal. Chem. 71 (1999) 928.
- [9] D.E. Cherrak, S. Khattabi, G. Guiochon, J. Chromatogr. A 877 (2000) 109.
- [10] F. Charton, S.C. Jacobson, G. Guiochon, J. Chromatogr. 630 (1993) 21.
- [11] L.S. Pais, J.M. Loureiro, A.E. Rodrigues, J. Chromatogr. A 827 (1998) 215.
- [12] K. Miyabi, G. Guiochon, Anal. Chem. 71 (1999) 889.
- [13] W. Rudzinski, D.H. Everett, Adsorption of Gases on Heterogeneous Surfaces, Academic Press, New York, NY, 1992.
- [14] M. Jaroniec, R. Madey, Physical Adsorption on Heterogeneous Solids, Elsevier, Amsterdam, The Netherlands, 1990.